Volume 78, Numbers 1 and 2 January/February 2008

Journal of Sedimentary Research

An International Journal of SEPM
(Society for Sedimentary Geology)

Journal of Sedimentary Research

Journal of Sedimentary Research, 2008, v. 78, 69–76
Research Article
DOI: 10.2110/jsr.2008.013

RECONSTRUCTION OF WATER TEMPERATURE, pH, AND FLUX OF ANCIENT HOT SPRINGS FROM TRAVERTINE DEPOSITIONAL FACIES

JOHN VEYSEY, II,[1] BRUCE W. FOUKE,[2] MICHAEL T. KANDIANIS,[2] THOMAS J. SCHICKEL,[2] ROY W. JOHNSON,[2] AND NIGEL GOLDENFELD[1]

[1]*Department of Physics, University of Illinois at Urbana-Champaign, 1110 West Green Street, Urbana, Illinois 61801-3080 U.S.A.*
[2]*Department of Geology, University of Illinois Urbana-Champaign, 1301 West Green Street, Urbana, Illinois 61801-3080 U.S.A.*
e-mail: fouke@uiuc.edu

ABSTRACT: **An extensive data set of the physical and chemical attributes of two modern hot springs in the Mammoth Hot Springs complex of Yellowstone National Park, Wyoming, U.S.A., yields a strong correlation between travertine depositional facies and the temperature, pH, and flux of the hot-spring water from which the travertine precipitated. Because advection dominates in these hot-spring drainage systems, we quantify variability between and within springs in order to construct a hydrologic model that defines the primary flow path in the context of key macroscopic travertine accumulation patterns. This model, based on 343 *in situ* triplicate measurements, provides the basis for the use of travertine facies models to quantitatively reconstruct hot-spring aqueous temperature, pH, and flux solely from precipitated travertine. As an example reconstruction, we deduce that previously described Pleistocene apron and channel facies travertine quarry deposits from central Italy precipitated from hot-spring waters with a pH of 6.86 ± 0.19 and a temperature of 65.4 ± 3.6°C.**

INTRODUCTION

The concept of a ***sedimentary depositional facies*** serves as a fundamental means for reconstructing aqueous paleoenvironments from the geological record. However, the facies concept itself is broadly defined, contains many assumptions about the physics, chemistry, and biology of the environment of deposition, and spans multiple temporal and spatial scales (Flügel 2004; Wilson 1975). Therefore, despite the universal familiarity of geoscientists with sedimentary depositional facies, there are significant variations in how the term facies is actually interpreted and applied in the literature.

The classic definition of a facies is based solely on a specific suite of solid-phase characteristics of a sedimentary rock (Gressly 1838; Reading 1996) and is determined exclusively by the grain and crystal chemistry, mineralogy, structure, fabric, shape, size, and overall gross morphology of the deposit. This original classical definition of a facies has since been broadened significantly in recent years to include the environmental conditions *believed* to have been present during formation of a specific sedimentary deposit (Walker 1984). This newer broadly interpretive sense of the word "facies" implicitly assumes that a modern analog has been analyzed where the same sedimentary deposit has been directly linked with a specific suite of environmental conditions. While many modern sedimentary facies have been qualitatively correlated with generalized ranges in environmental conditions (i.e., relative water depth, temperature, velocity, etc.), few studies have quantitatively measured and correlated key aqueous characteristics (i.e., specific water temperature, pH, flux, etc.) with classically defined depositional facies.

In the present paper, we directly address the problem that the key aqueous parameters of temperature, pH, and flux have not previously been quantitatively correlated with classically defined travertine depositional facies in a modern hot-spring system. This has in turn prevented the quantitative reconstruction of ancient hot-spring temperature, pH, and flux from specific fossil travertine facies deposits. Many previous studies have simultaneously analyzed hot-spring water and the travertine that it precipitates from both field and laboratory settings (see extensive review in Pentecost 2005). Furthermore, several of these studies propose differing versions of a travertine facies model, all of which assume many aspects of the environment that are never quantitatively measured (see exhaustive summary in Chapter 4 of Pentecost 2005). The goal of this study is therefore to establish the first quantitative correlation of a classically defined hot-spring travertine facies model with aqueous parameters that strongly influence travertine calcium carbonate precipitation.

Our research at Mammoth Hot Springs, Yellowstone National Park, Wyoming, U.S.A., quantifies the depositional environment within the context of a classically defined five-component travertine facies model originally described in Fouke et al. (2000). These five facies have been observed throughout the world (e.g., Rapolano Terme, in Tuscany, Italy; Fouke 2001) and are thus not unique to Yellowstone. With progression downstream from the source vent, the facies include the vent, apron and channel, pond, proximal-slope, and distal-slope, and are defined by their specific crystalline chemistry, mineralogy, structure, fabric, shape, size, and overall gross morphology (Fouke et al. 2000). Each of these depositional facies includes unique travertine features on all length scales. Because different processes influence carbonate precipitation at each scale, we have conducted our analyses within the following spatial hierarchy: (1) "microscopic" on the scale of microns to millimeters; (2) "mesoscopic" on the scale of millimeters to centimeters; (3) "macroscopic" on a scale of centimeters to meters; and, (4) "system level" on the scale larger than tens of meters. The upper limit of the systems level scale is determined by the area over which spring water precipitates travertine, and can range from approximately 50 to 500 meters at Mammoth (Bargar

 1527-1404/08/078-069/$03.00

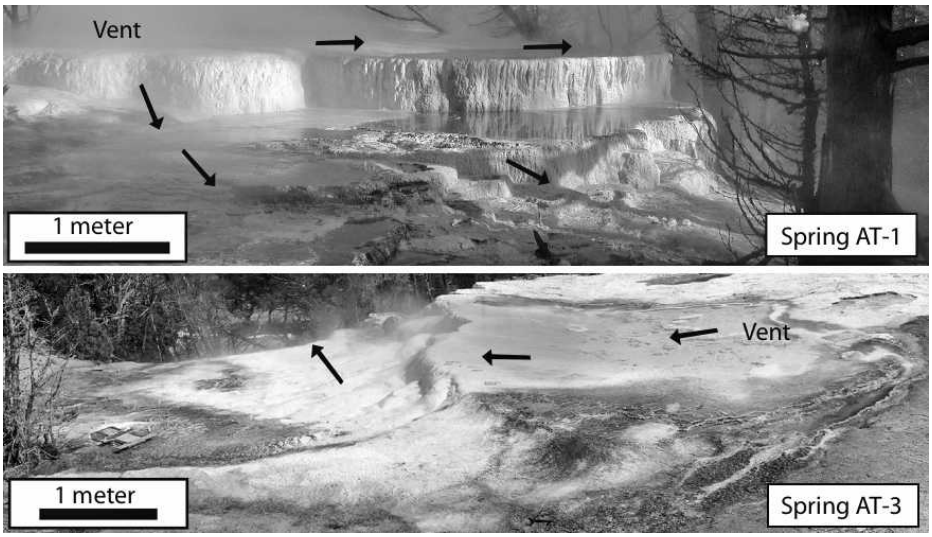

FIG. 1.—Spring AT-1 and AT-3 showing vent and general direction of spring-water flow.

1978) to almost a kilometer in other hot-spring systems around the world (Ford and Pedley 1996; Pentecost 2005).

In the present paper, we show that spring-water pH, temperature, and flux are sufficient to differentiate macroscopic patterns in calcium carbonate crystallization. We do this by quantifying fluctuations in these parameters and demonstrating that they are strongly correlated with the underlying depositional facies. We also define the concept of a primary flow path as a means of connecting the macroscopic aqueous environment to smaller length scales. These new results rigorously justify using classically defined facies travertine models to characterize hot-spring depositional environments, and demonstrate that they may be used to universally reconstruct the pH, temperature, and flux of equivalent recent and ancient hot springs environments.

GEOLOGIC SETTING

Mammoth Hot Springs, which lies on the northern flank of the Yellowstone caldera, contains a succession of travertine deposits that range from 0 to approximately 8,000 years old that are 73 m in thickness and cover more than 4 km^2 (Allen and Day 1935; White et al. 1975; Bargar 1978; Sturchio et al. 1992; Sturchio et al. 1994). The springs expel Ca–Na–HCO_3–SO_4 type hot waters derived from a subsurface reservoir at temperatures of greater than 100°C (Kharaka et al. 1991; Sorey 1991). Angel Terrace, near the top of the Mammoth complex, contains several active small springs. We have focused on two of these, AT-1 (described by Fouke et al. 2000 and Fouke et al. 2003) and AT-3, which are shown in Figure 1. The hydrologic system is dynamic, with multiple vents appearing, sealing, and reopening on Angel Terrace at a frequency of months to tens of years (Bargar 1978; Sorey 1991). The cessation of flow of AT-1 led to our subsequent study of Spring AT-3, which is located 100 m to the northeast of AT-1.

APPLYING THE CARBONATE-HOT-SPRING FACIES MODEL TO SPRING AT-3

The floor of the Spring AT-3 drainage system is composed of a sequence of morphologically distinct travertine deposits that can be consistently identified in the field at the mesoscopic, macroscopic, and system-level scales of observation. The AT-3 travertine deposits are consistent in crystalline form and fabric to the five travertine depositional facies originally described at AT-1 (Fouke et al. 2000). These include: (1) the vent facies, (2) the apron and channel facies, (3) the pond facies, (4) the proximal-slope facies, and (5) the distal-slope facies (see fig. 2 in Fouke et al. 2000). The travertine morphologies constituting each facies at AT-1, and now AT-3, as well as the relative succession of the facies along the drainage outflow, have been observed in other springs around the world and are consistently re-established as the springs shift their position due to changes in spring water flow velocity and the opening or closing of new vents (Fouke et al. 2000; Fouke et al. 2003; Fouke 2001).

A description of the travertine facies and their distribution within the Spring AT-3 drainage system is briefly summarized and presented in Table 1. The vent facies is composed of aragonite needle botryoids that form mounded travertine deposits up to 5 cm in height and 30 cm in diameter (Fig. 2A). The vent facies gradually passes laterally into the apron and channel facies, which is floored by hollow travertine tubes (called "streamers") that are composed of aragonite needle encrustations of filamentous thermophilic bacteria (Fig. 2B). The apron and channel facies at Spring AT-3 has prograded laterally over a previously formed large step-like morphology called a *terracette*, thus creating a waterfall within the apron and channel facies (Fig. 2B, C). This type of lateral progradation of travertine facies belts is consistently observed when the rate of spring water being discharged from the vent increases, resulting in lateral progradation and associated down-slope shifts in the lateral position of the facies downstream of the vent. The transition from the apron and channel facies to the pond facies is an abrupt contact associated with a dramatic drop in aqueous flux as the spring water slows and pools. Travertine in the pond facies terracettes (Fig. 2C) is composed of aragonite needle shrubs at higher temperatures and ridged networks of calcite and aragonite at lower temperatures. The proximal-slope facies abruptly begins at the margins (or lips) of the pond pools (terracettes, Fig. 2C, D). Proximal-slope travertine is composed of arcuate aragonite needle clusters that create small fluted microterracettes on the steep slope face (Fig. 2C, D). Finally, a gradual transition takes place into the distal-slope facies, where travertine forms broad low-relief microterracettes that are composed entirely of calcite spherules and "feather" calcite crystals.

CHARACTERIZATION OF SPRING WATER

Correlation of the solid-phase travertine facies with the spring water has required quantification of physical and chemical aqueous parameters within a complex, heterogeneous natural environment that exhibits large spatial variations and temporal fluctuations. Over a period of several years, our research group has collected measurements of the physical, chemical, and biological properties of two hot springs (AT-1 and AT-3) at Angel Terrace. During the course of the study, AT-1 stopped flowing in March 2004, necessitating that subsequent experiments be performed at AT-3. Our National Park Service research permit allowed access to only

TABLE 1.—*The characteristics of hot spring travertine that* ***define*** *the five component depositional facies model used to analyze AT-1 and AT-3 (Fouke et al. 2000.) Each facies definition is based on features at multiple length scales.*

Level of description	Facies				
	Vent	Apron Channel	Pond	Proximal Slope	Distal Slope
Microscopic ***(μm–mm)***	Botryoidal aragonite needles (< 100 μm).	Botryoidal aragonite needles (< 100 μm) encrusting hollow tubes of microcrystalline calcite.	Aragonite needles (< 100 μm) arranged into dendritic shrubs or "fuzzy dumbbells" or microcrystalline calcite (50–100 μm).		Blocky calcite (25–100 μm) forming dendritic clusters (feather crystals) and spherulites.
Mesoscopic ***(mm–cm)***	Botryoids encrust each other, forming mushroom shaped hemispherical mounds.	A pavement composed of tightly bundled carbonate tubes a few millimeters to 10s of centimeters in length.	Shrubs aggregated into "cotton balls" or ridged networks with calcite ice sheets and calcified bubbles.	Microterracette calcite ice sheets, calcified bubbles.	Calcite shrubs, spherulites, and bubbles.
Macroscopic ***(cm–m)***	Bowl-shaped depression (< 0.5 m deep). Very well indurated.	A gently sloped channel floored by a well indurated pavement.	Multiple semicircular connected depressions (ponds), rimmed on one side by a thin lip (dam) with a scalloped face.	Multiple meter-scale rounded, scalloped mounds.	Low-profile elongated, connected depressions (ponds) with thick, rounded, lips and scalloped faces.
Systems level ***(> 10 m)***	Single contiguous area adjacent to apron channel. Thickest local deposits of travertine.	Single contiguous area adjacent to vent.	Not adjacent to vent. Not found on steep slopes.	Not adjacent to vent. Found on steep slopes.	A calcite region adjacent to aragonite. Not adjacent to vent or apron channel. Thinnest local travertine deposits.

one spring at a time, precluding simultaneous comparative analyses between AT-1 and AT-3.

The springs were surveyed using a Brunton compass, a 30 m steel tape measure, and a Garmin Model 12 GPS unit. The locations of all sample sites were determined with respect to the vent. During each trip, samples were collected along *transects*, defined as groups of measurements taken at nearly the same time at locations beginning with the vent and proceeding downstream through the drainage system. All measurements were taken in triplicate; the mean is taken as our best estimate of the true value, and the standard deviation quantifies measurement uncertainty.

We collected 343 pH measurements *in situ*, using three types of temperature correcting hand held probes: a Hach sensION 156 meter; an Orion Model 290A probe; and an Oaktron Waterproof Series 300 meter. Different meters were needed because the spring environment rapidly degrades and destroys probes. The meters were calibrated before, during, and after each transect using standard pH buffer solutions (4.0, 7.0, and 10.0) with an accuracy of ± 0.01 pH at 25°C. pH measurements were complicated because of the rapid deposition of $CaCO_3$ on the probes' electrodes. In order to avoid instrument drift and slow convergence to a steady measurement, the probes were regularly steeped in a 0.1M HCl solution, rinsed in deionized water, and then recalibrated.

Measurements of water temperature were taken at the same times and locations as pH measurements, using the same probes. Temperature was also collected every 30 seconds *in situ* using two Hobo Temperature Data loggers (Model H20-001).

Total flux in spring AT-3 was determined at the vent source using a propeller-based current meter, U.S.G.S. Pygmy Meter Model 6205, and by measuring the area through which current was flowing. The total flux at AT-1 was not measured because we could not reach the vent source with our current meter. We obtained an independent measure of flux at AT-3 using time-of-flight techniques inside a channel which had a fixed cross sectional area. This method records the length of time over which small, floating travertine flakes need to travel a given distance. The pygmy meter was also used to characterize typical flow velocities in the spring system and, where possible, Pitot tubes were used to validate these measurements.

DEFINITION OF THE PRIMARY FLOW PATH

To connect macroscopic processes to those which control precipitation at a microscopic scale, we followed the evolution of spring water as it progressed along a single *flow path* (using a Lagrangian frame of reference). A flow path is the set of points traversed by a packet of water as it moves from the vent to the distal slope. In a hot spring, unlike in a stream or river, there are multiple flow paths. Given a contiguous area covered by spring water, the primary flow path is the set of points at a given distance from the vent which are traversed by the largest volume of water. While the primary flow path can sometimes be identified by visual inspection, this is not always the case, particularly in thin sheet flow farther away from the vent. In this situation the primary flow path locally follows the trajectory along which temperature decreases most slowly as a function of distance.

Consider the contour of all points which are the same distance, $|\Delta\vec{r}|$, from the last identified point on the flow path, which we denote $\vec{r}_0$. If we are looking nearby, $|\Delta\vec{r}|$ must be small, and all these points will have the same water depth, H. In most of our system, this is a good approximation even for non-infinitesimal $|\Delta\vec{r}|$. If $v(\vec{r})$ is the local velocity, and $\Delta\vec{s}$ a small displacement along the equidistant contour, then flux $Q(\vec{r}_0 + \Delta\vec{r})$ at each of these points can be estimated as follows:

$$Q(\vec{r}_0 + \Delta\vec{r}) = H\Delta\vec{s}v(\vec{r}_0 + \Delta\vec{r}) \propto v(\vec{r}_0 + \Delta\vec{r}) \approx \frac{\Delta\vec{r}}{\Delta t} \quad (1)$$

Here Δt denotes the time it takes a packet of water to go from $\vec{r}_0$ to $\vec{r}_0 + \Delta\vec{r}$. Because the points being considered are equidistant, $Q(\vec{r}_0 + \Delta\vec{r}) \propto \frac{1}{\Delta t}$. Until the water packet reaches thermal equilibrium with the atmosphere, temperature decreases monotonically as a function of time, regardless of position or distance from the source. Hence $T = f$

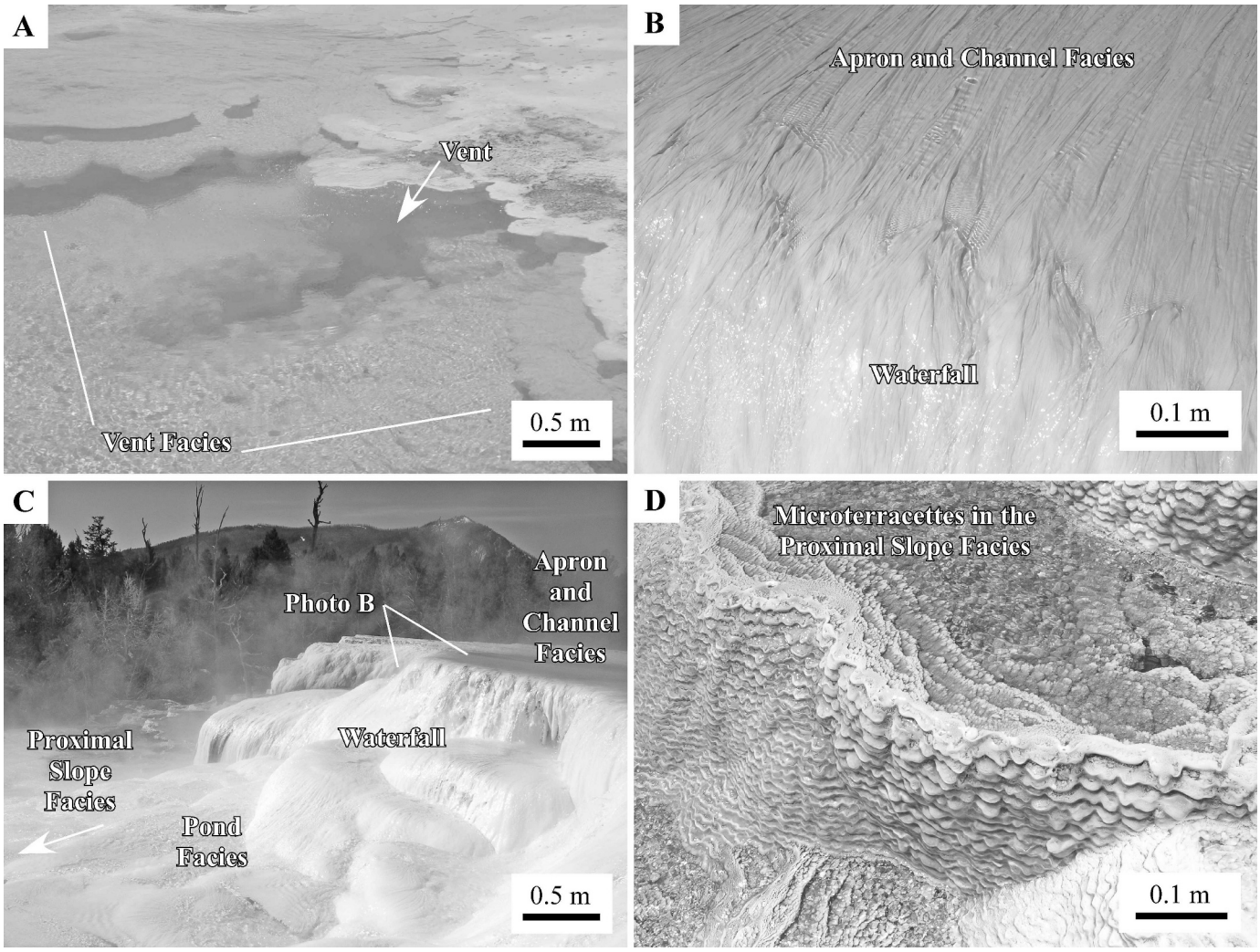

FIG. 2.—Field photographs of the travertine depositional facies observed at Spring AT-3. The downstream vent sequence of the travertine facies at Spring AT-3 (i.e., vent, apron and channel, pond, proximal-slope, distal-slope), as well as the centimeter-scale crystalline fabric constituting each facies deposit (as described in Table 1), is consistent with those that were observed being deposited in Spring AT-1 by Fouke et al. (2000). **A)** View of the Spring AT-3 vent within the vent facies. **B)** Travertine "streamer" fabrics constituting the apron and channel facies. Viewpoint of photograph is shown in photo C. **C)** Contacts between the apron and channel, pond, and proximal-slope facies. **D)** Proximal-slope facies, including microterracette dams.

(t) as the water packet moves from $\vec{r}_0$ to $\vec{r}_0 + \Delta\vec{r}$. If $|\Delta\vec{r}|$ is sufficiently small, then Δt must also be small. By expanding $f(t)$ for small Δt, we can write $\Delta t \propto \Delta T$, which implies that:

$$Q(\vec{r}_o + \Delta\vec{r}) \propto \frac{1}{\Delta T} \tag{2}$$

Hence, $Q(\vec{r}_o + \Delta\vec{r})$ will be maximized where ΔT is minimized. The next point on the primary flow path will be the spot among these equidistant points with the smallest ΔT, or equivalently the spot with the highest temperature. Thus, the primary flow path locally follows the trajectory along which temperature decreases most slowly as a function of distance. This theoretical discussion was applied to the data collected at spring AT-3, and the primary flow path was determined by looking at the average temperatures at the 24 sample locations throughout the spring. Figure 3 shows that the points which comprise the primary flow path locally minimize $d\mathrm{T} / d\mathrm{r}$.

This analysis provides a useful framework for analyzing aqueous measurements and for organizing experiments at hot springs. If one proceeds downstream with a meter stick and a thermometer, and draws arcs with the meter stick, the next point in the flow path will be the point along the arc with the highest temperature. When combined with standard qualitative observations, this approach allows sampling strategies which account for mixed flow paths, regardless of variations in water depth, velocity, or changes in underlying topography.

VARIABILITY AND FLUCTUATIONS IN HOT-SPRING WATER

Table 2 compares the ranges of observed water temperatures and pH, as a function of facies, for multiple hot springs and times. There is consistent overlap between readings from the same facies at different springs (AT-1 and AT-3), but there are also large variations within each facies. Although we observed variations in spring-water temperature and pH, the overall downflow trends were discernible. The identification of more meaningful differences that existed between and within the hot springs, however, required us to quantify the macroscopic fluctuations and variations that occurred within a single spring.

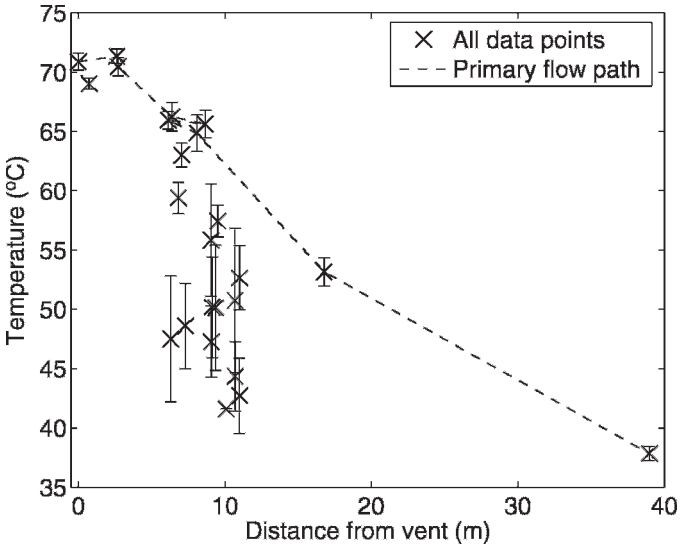

FIG. 3.— Temperature data from Spring AT-3. Each point represents the average of five triplicate measurements at each of 24 sample locations, taken over a period of three days. The primary flow path, represented by the dotted line, was determined using Equation 2, and locally minimizes dT / dr.

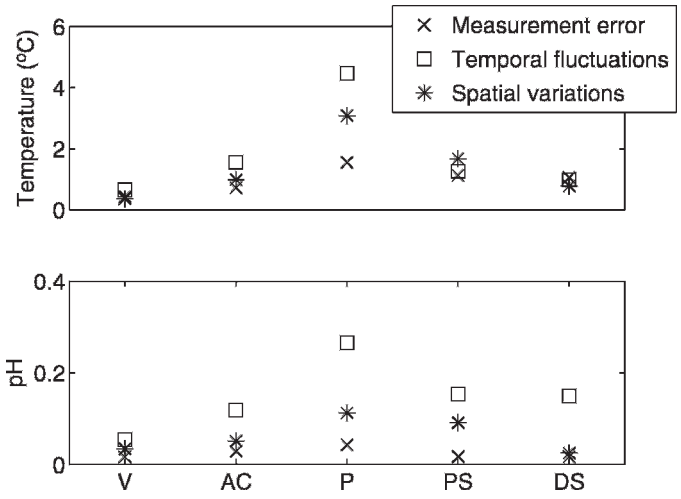

FIG. 4.— The three kinds of variability relevant to understanding travertine deposition in comparing hot springs, organized by facies. These include the vent facies (V), apron and channel facies (AC), pond facies (P), proximal-slope facies (PS), and the distal-slope facies (DS).

Three kinds of variability are relevant to carbonate precipitation. First, there are temporal fluctuations on the time scale of our measurements (e.g., tens of seconds). In our error model, these fluctuations are treated as measurement errors. Second, there are temporal fluctuations on the time scale of days, such as changes in spring discharge. These are relevant for comparing different measurements but not for understanding travertine deposits thicker than a few millimeters. Finally, there are spatial variations on the macroscopic scale. There are also spatial differences on both the microscopic and system-level scale but these are irrelevant to the scope of this discussion.

Figure 4 shows these three kinds of temporal and spatial variability for both temperature and pH as a function of facies. We quantified temporal fluctuations by considering the ensemble of measurements at a given point in space (taken over a period of three days), calculating the standard deviation of that ensemble, and then averaging those deviations over each facies. We quantified spatial variations by grouping all measurements collected within a facies at a given time, and then calculating the standard deviation of that ensemble. This was repeated for measurements taken at different times, and the results were averaged over each facies.

Although the measurement errors were small (approximately ± 0.03 pH units and ± 1°C), the temporal fluctuations and spatial variations were more significant. These differences could not be due to large changes in the source water, in as much as the vent exhibits the smallest changes. Both fluctuations and variations result from the interplay of many smaller factors including changes in the flow patterns upstream from a point, diurnal insolation, changes in total spring flux, and atmospheric conditions like wind. Specifically, in areas of low flux, we observed wind driving water over the pond lips and causing dramatic changes in the pH and temperature of downstream points.

Two HOBO temperature data loggers were deployed for three days in the proximal slope and pond facies (Fig. 5). The proximal slope measurements recorded a maximum change of ± 9°C, with a standard deviation of ± 2°C, and exhibited a clear diurnal signal, driven by differences in daytime and nighttime air temperatures as large as 20°C. The fluctuations seen in the HOBO data are consistent with the results shown in Figure 4.

Total spring-water flux was considerably more difficult to measure than either temperature or pH. In June 2004, using a pygmy current meter, we estimated Spring AT-3 discharge at 59 L/s. In January 2005, using time of flight techniques, we measured 12 L/s. Both measurements are accurate to within ± 10%. These numbers indicate significant variation in total spring flux, which will result in changes in downstream

TABLE 2.—*Temperature and pH ranges for each of the previous studies for springs AT-1 and AT-3. Studies are organized by year and facies. Temperature (°C) is listed on top of pH in each row.*

Year	Spring Location	Value	Vent Facies	Apron and Channel Facies	Pond Facies	Proximal-Slope Facies	Distal-Slope Facies
2005	AT-3	T (°C)	69.6	64.1	N/A	47.2	34.1
		pH	6.29	6.62		7.76	8.14
2004	AT-3	T (°C)	68.0–72.2	60.5–68.6	35.6–61.7	50.6–56.4	34.2–39.4
		pH	6.21–6.57	6.59–7.26	6.84–8.04	6.99–7.77	7.32–8.07
2003	AT-3	T (°C)	71.2	61.6–69.3	56.1–61.5	41.3–65.2	28.4–44.0
		pH	6.58–6.61	6.60–7.05	6.94–7.01	7.04–8.01	7.75–8.14
2002	AT-1	T (°C)	67.9–69.3	60.5–64.0	59.9–60.3	46.7–50.8	24.0
		pH	6.59–6.76	7.00–7.26	7.29–7.30	7.95–8.05	8.12
1999	AT-1	T (°C)	72.0–72.2	70.1–70.3	46.8–55.3	39.0–39.8	37.1–37.5
		pH	6.31–6.32	6.46–6.52	7.42–7.62	7.73–7.77	7.90–7.92
1998	AT-1	T (°C)	73.2	N/A	45.3	54.2	30.2
		pH	6.00		7.43	7.40	8.00

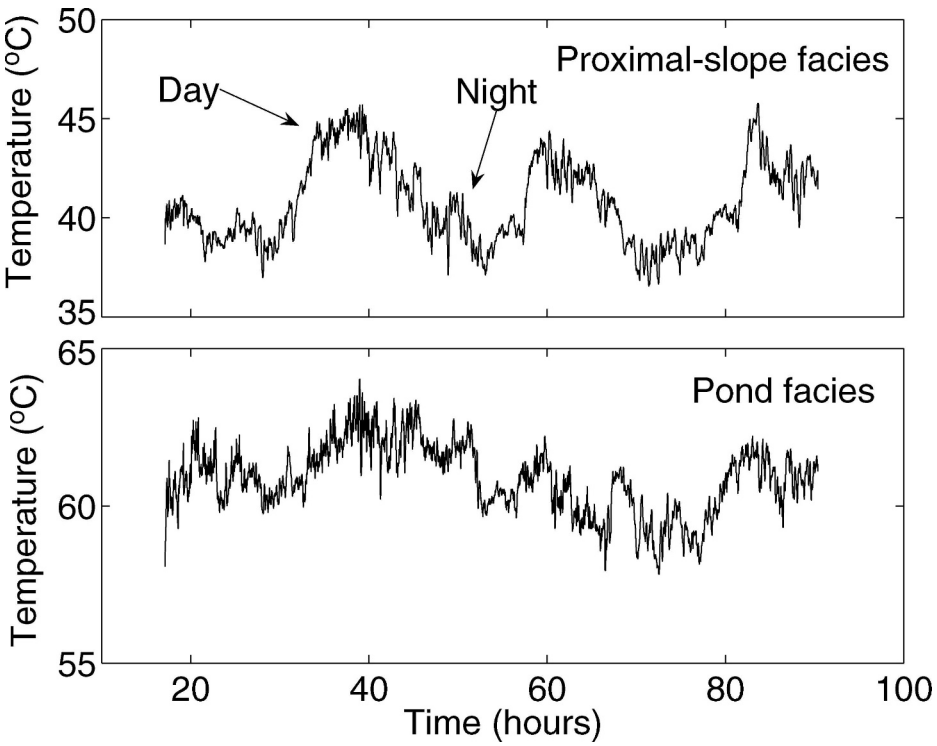

FIG. 5.—Three days worth of HOBO temperature data from spring AT-3. The data loggers recorded a measurement every 30 s. The bottom plot shows results from a pond facies, and the top plot data from a relatively cool point in the proximal slope facies.

aqueous chemistry, temperature, and flux even if the source water remains otherwise unchanged. Our water-flux measurements do not agree with the report of Sorey (1991), who reported the total discharge of all hot springs in the Mammoth complex as 59.1 ± 3 L/s.

Figure 4 shows a noteworthy trend in spatial variability. The largest heterogeneities in temperature and pH are seen in the pond facies, and the most homogeneous regions are the vent and distal-slope facies. This occurs because the spring system is held fixed at the beginning and the end of the primary flow path. At the vent, pH and temperature are held constant by the steady influx of homogeneous source water, which has relatively constant temperature and chemistry (Table 2). Far from the source, water temperature and CO_2 fugacity asymptotically approach equilibrium with both the atmosphere and solid $CaCO_3$ in the substrate. The small precipitation rates in the distal slope facies (Fouke et al. 2000) indicate that the spring water is nearing equilibrium, a fact which explains decreased spatial variations in pH. The temporal fluctuations in temperature exhibit the same trend. They are initially small in the vent facies, rise until the pond facies, and then decrease.

RELATING THE ROCK RECORD TO THE DEPOSITIONAL ENVIRONMENT

Despite large variations and fluctuations in the aqueous environment, we see statistically significant correlations between physical and chemical attributes of spring water and underlying depositional facies. These correlations exist because macroscopic $CaCO_3$ mineral precipitation occurs on time scales of days to months, and the rock record inherently averages out more rapid fluctuations in the aqueous environment.

Figure 6 shows the distribution of all pH and temperature measurements arranged by facies. It illustrates that the vent, apron and channel, and distal-slope facies can be identified by considering pH and temperature jointly, implying that these facies are associated with distinct depositional environments. A Kruskal-Wallis non-parametric test shows these distinctions to be statistically significant, as detailed in the Supplementary Material (see Acknowledgments section for URL). The transition from the vent to the apron and channel facies is associated with the pH increasing beyond 6.6 while temperature is relatively unchanged. This is consistent with this transition being controlled by CO_2 exsolution and the onset of carbonate precipitation.

The pond and proximal-slope facies cannot be differentiated from each other on the basis of water temperature and pH (see Supplementary Material). Although petrography documents some similarity on a microscopic level (Fouke et al. 2003; Fouke et al. 2000), clear distinctions (such as travertine dams and a terraced architecture) emerge on a macroscopic level. We therefore considered additional physical parameters to understand how the same spring water can give rise to two distinct aggregate morphologies. These two facies are differentiated by average fluid flux.

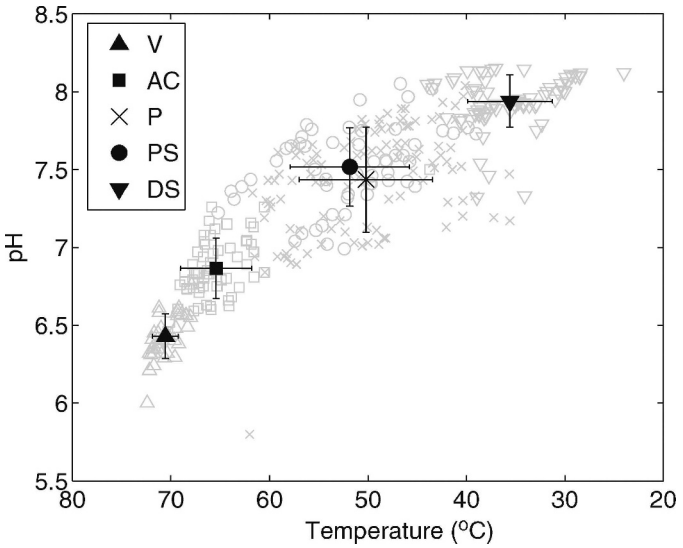

FIG. 6.—The distribution of 343 triplicate pH and temperature measurements taken from Springs AT-1 and AT-3 at different times. The black symbols show the facies averages, with the error bars denoting one standard deviation.

Velocities in these thin sheet flows are difficult to measure, particularly because techniques like particle image velocimetry could negatively impact the natural hot-spring environment. We have used several independent techniques, including the pygmy current meter, Pitot tubes, and time-of-flight measurements. Typical velocities of less than 20 cm/s were observed in the pond but over 35 cm/s in the proximal-slope. The average velocities in these facies are a function of slope, total flux, fluid depth, and facies area. Using our measurements of area, depth, and total flux, we calculate velocities consistent with these experimental findings. Our observations suggest that, when other factors remain unchanged, ponds form in flatter areas with lower flux and the proximal-slope facies form on steeper underlying topographies with higher flux. This macroscopic pattern is seen at both springs, and is independently supported by computational models of these hot-spring systems that simulated macroscopic travertine pattern formation and showed terracette-like structures where velocities were slower (Goldenfeld et al. 2006). As the spring landscape evolves, both flux and slope change as a result of travertine deposition. This can result in a steep proximal-slope ultimately becoming terraced ponds.

RECONSTRUCTING MODERN AND ANCIENT ENVIRONMENTS

The strong correlations between travertine facies and the macroscopic physical and chemical parameters of the depositional environment allow each facies to be uniquely identified solely by pH, temperature, and flow velocity. Although fluctuations and variations complicate comparisons between springs, we have shown that when viewed statistically (Fig. 6), measurements taken from the same facies in different springs are equivalent. It cannot be overemphasized that this applies only to specific depositional facies, those defined by Fouke et al. (2000). The mineral deposits used in these facies definitions can be formed only at carbonate hot springs whose source water is sufficiently similar.

When combined with previous work (Fouke et al. 2000 and Fouke et al. 2003), these results demonstrate that these travertine depositing hot springs exhibit the same macroscopic partitions chemically, physically, petrographically, and microbially. Other studies that report hot-spring temperature and pH in the context of aggregate morphology (Chafetz and Lawrence 1994) are consistent with the geochemical partitions shown in Figure 6. Note that cooler carbonate springs which have significantly different source water temperature will not develop the same five facies, and are therefore not comparable.

This simple linkage is a powerful predictive tool, implying that our hot-spring travertine facies model, which inherently averages fluctuations and variations, can be used directly for paleoenvironmental reconstructions of water temperature, pH, and flux. Our results also put quantitative bounds on the temperature and pH of the spring water from which ancient travertine facies originally precipitated, as long as care is taken in using the rigorous classical approach of defining the depositional facies.

To accurately categorize ancient fabrics, we must use the fact the Fouke et al. (2000) and Fouke et al. (2003) facies model is defined at several scales (Table 1, Fig. 4). The vent and apron and channel facies can be identified with confidence based on only their distinctive macroscopic characteristics. Pond and proximal-slope facies can be recognized by using either microscopic, mesoscopic, and macroscopic details or by combining macroscopic and system-level observations. Ancient distal-slope facies are the hardest to identify, requiring a combination of all four levels of description.

As an example, Folk et al. (1985) documented streamers (Fig. 2B) in Pleistocene travertine, primary crystallization features which were preserved despite subsequent post-depositional physical and chemical alterations (diagenesis; Bathurst 1975). This macroscopic fabric, a distinctive pavement composed of aragonite-encrusted filaments, is seen only in the apron and channel facies at high temperature carbonaceous springs. Therefore, utilizing Figure 6, we conclude that these deposits precipitated from waters with a pH of 6.86 $\pm$ 0.19 and a temperature of 65.4 $\pm$ 3.6°C.

CONCLUSIONS

A comprehensive set of measurements of hot-spring water temperature, pH, and flux were quantitatively correlated with classically-defined travertine depositional facies at two carbonate hot springs in Yellowstone National Park. Although the aqueous environment of these terrestrial carbonate hot springs exhibits large spatial variations and temporal fluctuations on the macroscopic scale, our data reveal that water pH, temperature, and flux are sufficient to associate spring water directly to the depositional facies. The observed strong correlations between travertine facies and the spring water explicitly link these travertine facies with the aqueous environment from which they precipitated. This validates the classically defined travertine facies concept as a macroscopic framework for comparing modern hot springs and justifies the widespread application of the term "facies" to the environmental conditions believed to have been present during formation of a specific sedimentary deposit (Walker 1984). Finally, these results place more accurate quantitative bounds on paleoenvironmental reconstructions of water temperature, pH, and flux from ancient hot-spring travertine.

ACKNOWLEDGMENTS

This work was supported by research awards from the National Science Foundation Biocomplexity in the Environment Program (EAR 0221743), the American Chemical Society Petroleum Research Fund Starter Grant Program (34549-G2), and the University of Illinois Urbana-Champaign Critical Research Initiative. The conclusions of this study are those of the authors, and do not necessarily reflect those of the funding agencies. Thanks to G. Bonheyo, D. Fike, B. Sansenbacher, H. Garcia Martin, and K. Hutchings for assistance with data collection. We also thank A. Murray, A. Kameda, and B. Carter for field work, helpful comments, and HOBO temperature data. We are indebted to the National Park Service, particularly B. Suderman, H. Hessler, C. Hendrix, and C. Smith for their support, assistance, passion, and ongoing preservation of Yellowstone hot springs.

The Supplemental Material described in the paper can be found in JSR's Data Archive, <<http://www.sepm.org/jsr/jsr_data_archive.asp>>.

REFERENCES

Allen, E.T., and Day, A.L., 1935, Hot Springs of the Yellowstone National Park: Carnegie Institution of Washington, Publication 466, 525 p.

Bargar, K.E., 1978, Geology and thermal history of Mammoth Hot Springs, Yellowstone National Park, Wyoming: U.S. Geological Survey, Bulletin, v. 1444, p. 1–54.

Bathurst, R.G.C., 1975, Carbonate Sediments and their Diagenesis: Amsterdam, Elsevier, Developments in Sedimentology, v. 12, 658 p.

Chafetz, H.S., and Lawrence, J.R., 1994, Stable isotope variability within modern travertines: Géographie Physique et Quaternaire, v. 48, p. 257–273.

Flügel, E., 2004, Microfacies of Carbonate Rocks: Analysis, Interpretation, and Application: Berlin, New York, Springer, 976 p.

Folk, R.L., Chafetz, H.S., and Tiezzi, P.A., 1985, Bizarre forms of depositional and diagenetic calcite in hot-spring travertines, central Italy, *in* Schneidermann, P., and Harris, P.M., eds., Carbonate Cements: SEPM, Special Publication 36, p. 349–369.

Ford, T.D., and Pedley, H.M., 1996, A review of tufa and travertine deposits of the world: Earth-Science Reviews, v. 41, p. 117–175.

Fouke, B.W., 2001, Depositional facies and aqueous–solid geochemistry of travertine-depositing hot springs (Angel Terrace, Mammoth Hot Springs, Yellowstone National Park, U.S.A.)—Reply: Journal of Sedimentary Research, v. 71, p. 497–500.

Fouke, B.W., Farmer, J.D., Des Marais, D.J., Pratt, L., Sturchio, N.C., Burns, P.C., and Discipulo, M.K., 2000, Depositional facies and aqueous–solid geochemistry of travertine-depositing hot springs (Angel Terrace, Mammoth Hot Springs, Yellowstone National Park, U.S.A.): Journal of Sedimentary Research, v. 70, p. 265–285.

Fouke, B.W., Bonheyo, G.T., Sanzenbacher, B., Frias-Lopez, J., and Veysey, J., 2003, Partitioning of bacterial communities between travertine depositional facies at Mammoth Hot Springs, Yellowstone National Park, U.S.A.: Canadian Journal of Earth Sciences, v. 40, p. 1531–1548.

Goldenfeld, N., Chan, P.Y., and Veysey, J., 2006, Dynamics of precipitation pattern formation at geothermal hot springs: Physical Review Letters, v. 96, p. 45–49.

Gressly, A., 1838, Observations géologiques sur le Jura soleurois: Nouveaux mémoires de la Société Helvetique des Sciences Naturelles, Neuchâtel, v. 2, 349 p.
Kharaka, Y.K., Mariner, R.H., Bullen, T.D., Kennedy, B.M., and Sturchio, N.C., 1991, Geochemical investigations of hydraulic connections between Corwin Springs known geothermal area and adjacent parts of Yellowstone National Park, *in* Sorey, M., ed., Effects of Potential Geothermal Development in the Corwin Springs Known Geothermal Resources area, Montana, on the Thermal Features of Yellowstone National Park: U.S. Geological Survey, Water-Resources Investigations, Report 91-4052, p. F1–F38.
Pentecost, A., 2005, Travertine: Heidelberg, Germany, Springer-Verlag, 445 p.
Reading, H.G., 1996, Sedimentary Environments; Processes, Facies and Stratigraphy: London, Blackwell Science, 688 p.
Sorey, M.L., 1991, Effects of potential geothermal development in the Corwin Springs known geothermal resources area, Montana, on the thermal features of Yellowstone National Park: U.S. Geological Survey, Water-Resources Investigations, Report 91-4052, 110 p.
Sturchio, N.C., Murrell, M.T., Pierce, K.L., and Sorey, M.L., 1992, Yellowstone travertines: U-series ages and isotope ratios (C, O, Sr, U), *in* Kharaka, Y.K., and Maest, M.D., eds., Water–Rock Interaction, Rotterdam, Balkema, p. 1427–1430.
Sturchio, N.C., Pierce, K.L., Murrell, M.T., and Sorey, M.L., 1994, Uranium-series ages of travertines and timing of the last glaciation in the northern Yellowstone area, Wyoming–Montana: Quaternary Research, v. 41, p. 265–277.
Walker, R.G., 1984, Facies Models: St. Johns, Newfoundland, Geological Association of Canada, 317 p.
White, D.E., Fournier, R.O., Muffler, L.P.J., and Truesdell, A.H., 1975, Physical results of research drilling in thermal areas of Yellowstone National Park, Wyoming: U.S. Geological Survey, Professional Paper 892, 145 p.
Wilson, J.L., 1975, Carbonate Facies in Geologic History: New York, Springer-Verlag, 472 p.

Received 12 July 2006; accepted 16 August 2007.